Energy Materials

Low-concentrated sulfone electrolyte enables high-voltage chemistry of lithium-ion batteries

--Manuscript Draft--

Manuscript ID:	EM-2022-38
Manuscript Title:	Low-concentrated sulfone electrolyte enables high-voltage chemistry of lithium-ion batteries
Manuscript Type:	Article
Special Issue:	
Keywords:	Electrolyte, sulfone, fluorobenzene, interphase, lithium-ion battery
Corresponding Author(s):	Xiulin Fan
Corresponding Author' Email:	xlfan@zju.edu.cn
Corresponding Author's Department:	State Key Laboratory of Silicon Materials, School of Materials Science and Engineering
Corresponding Author's Institution:	Zhejiang University
Country/Region:	China
Order of Author (Only first three authors will be listed):	1
Author's Name:	Ling Lv
Order of Author:	2
Author's Name:	Haikuo Zhang
Abstract:	Commercial carbonate electrolytes with poor oxidation stability and high flammability limit the operation voltage of Li-ion batteries (LIBs) up to ~ 4.3 V. As one of the most promising candidates for electrolyte solvents, sulfolane (SL) has received great interest because of its wide electrochemical window, low flammability and high dielectric permittivity. Unfortunately, SL-based electrolytes with normal concentration cannot achieve highly reversible Li+ intercalation/de-intercalation in graphite anode due to an ineffective solid electrolyte interface (SEI), thus undermining its application in LIBs. Here, a low-concentrated SL-based electrolyte (LSLE) was developed for the high-voltage graphite||LiNi0.8Co0.1Mn0.1O2 (NCM811) full-cells. The highly reversible graphite anode can be achieved through the preferential decomposition of dual-salt LiDFOB-LiBF4 in LSLE. The addition of fluorobenzene (FB) further restrains the

	decomposition of SL, endowing uniform, robust and inorganic-rich interphases on the surface of electrodes. As a result, the LSLE with improved thermal stability can support the MCMB||NCM811 full-cells at 4.4 V, evidenced by an excellent cycling performance with capacity retentions of 83% after 500 cycles at 25 ℃ and 82% after 400 cycles at 60 ℃. We believe that the design of FB-containing LSLE offers an effective routine for next-generation low-cost and safe electrolytes of high-voltage LIBs.
Funding Agency and Grant Number:	

Supplementary Material

Low-concentrated sulfone electrolyte enables high-voltage chemistry of lithium-ion batteries

Ling Lv[a], Haikuo Zhang[a], Di Lu[a], Yuan Yu[b*], Jiacheng Qi[a], Junbo Zhang[a], Shuoqing Zhang[a], Ruhong Li[a],Tao Deng[c], Lixin Chen[a,d] and Xiulin Fan[a*]

[a]State Key Laboratory of Silicon Materials, School of Materials Science and Engineering, Zhejiang University, Hangzhou 310027, China. Email: xlfan@zju.edu.cn

[b]Zhejiang Provincial Key Laboratory of Fiber Materials and Manufacturing Technology, Zhejiang Sci-Tech University, Hangzhou 310018, China. email：yuyu@zstu.edu.cn

[c]Department of Chemical and Biomolecular Engineering, University of Maryland, College Park, MD, USA.

[d]Key Laboratory of Advanced Materials and Applications for Batteries of Zhejiang Province, Hangzhou 310013, China

Supplementary Table 1. Surface resistance (R_{SEI}), charge transfer resistance (R_{ct}) and interfacial resistance (R_i) of MCMB||NCM811 full-cells using different electrolytes corresponding to the EIS data of fitting equivalent circuit in Figure S8.

Electrolyte	R	Cycle		
		10th	50th	100th
LiDFOB-$LiBF_4$/SL-FB	R_{SEI} (Ohm)	39.4	0.9	1.3
	R_{ct} (Ohm)	262.4	100.9	101.8
	R_i (Ohm)	301.8	101.8	103.1
LiDFOB-$LiBF_4$/SL	R_{SEI} (Ohm)	24.3	1.3	0.7
	R_{ct} (Ohm)	248.1	111.2	127.7
	R_i (Ohm)	272.4	112.5	128.4
BE	R_{SEI} (Ohm)	37.8	1.2	1.4
	R_{ct} (Ohm)	303.6	134.7	144.4
	R_i (Ohm)	341.4	135.9	145.8

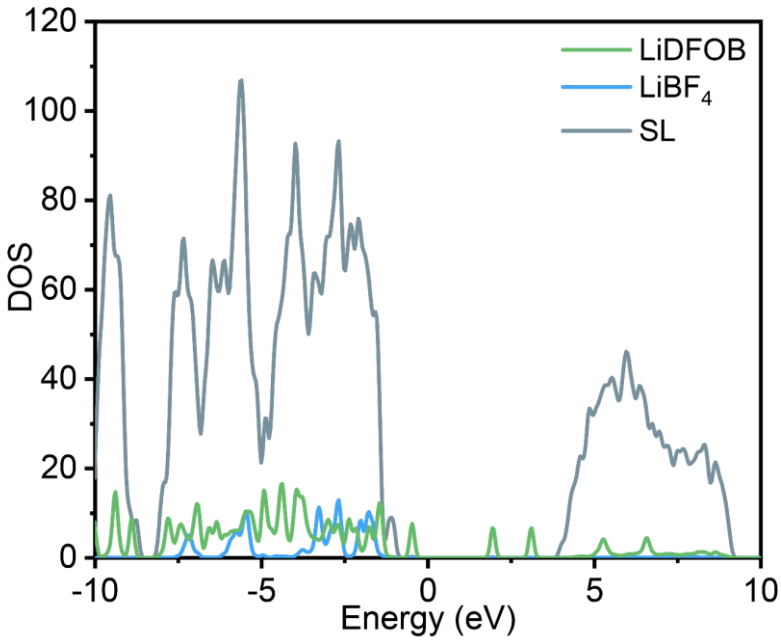

Figure S1. Density of states (DOS) obtained in quantum mechanical DFT-AIMD simulations of LiDFOB-$LiBF_4$/SL.

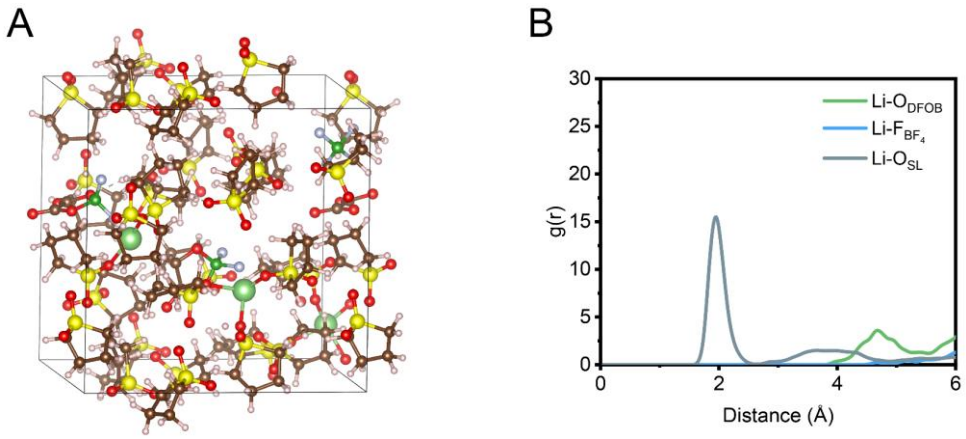

Figure S2. AIMD simulation results of LiDFOB-LiBF$_4$/SL electrolyte. (A) AIMD simulation snapshots of LiDFOB-LiBF$_4$/SL. (B) Radical distribution functions calculated from AIMD simulation of LiDFOB-LiBF$_4$/SL electrolyte.

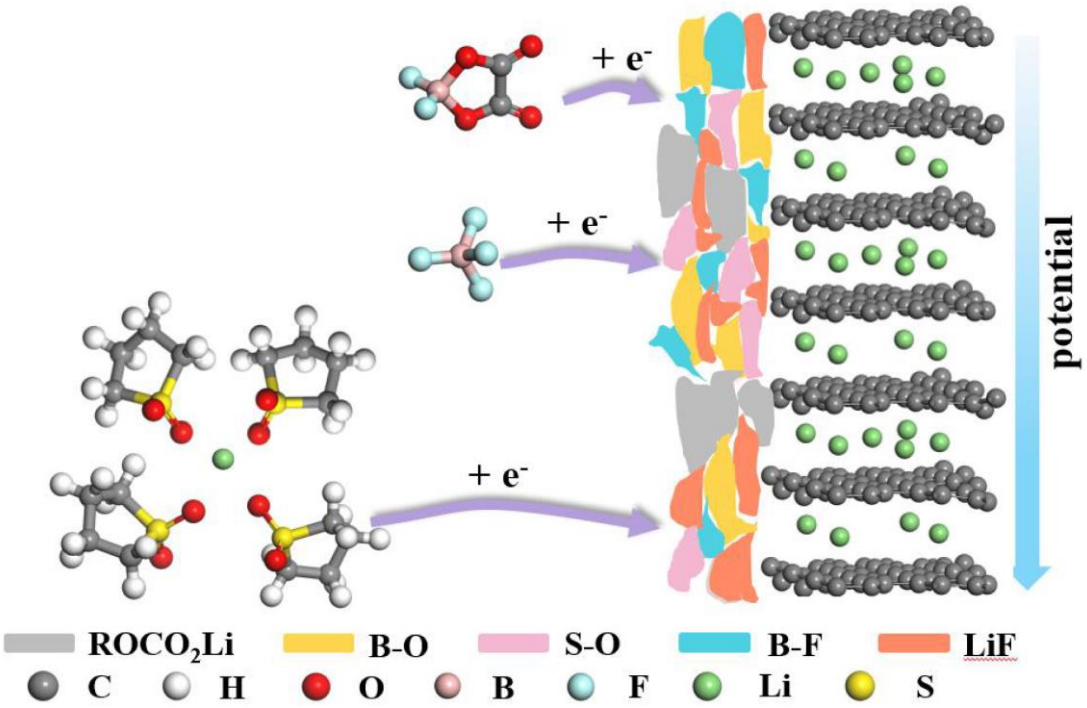

Figure S3. Schematic diagram of reaction at LiDFOB-$LiBF_4$/SL electrolyte /graphite interphase.

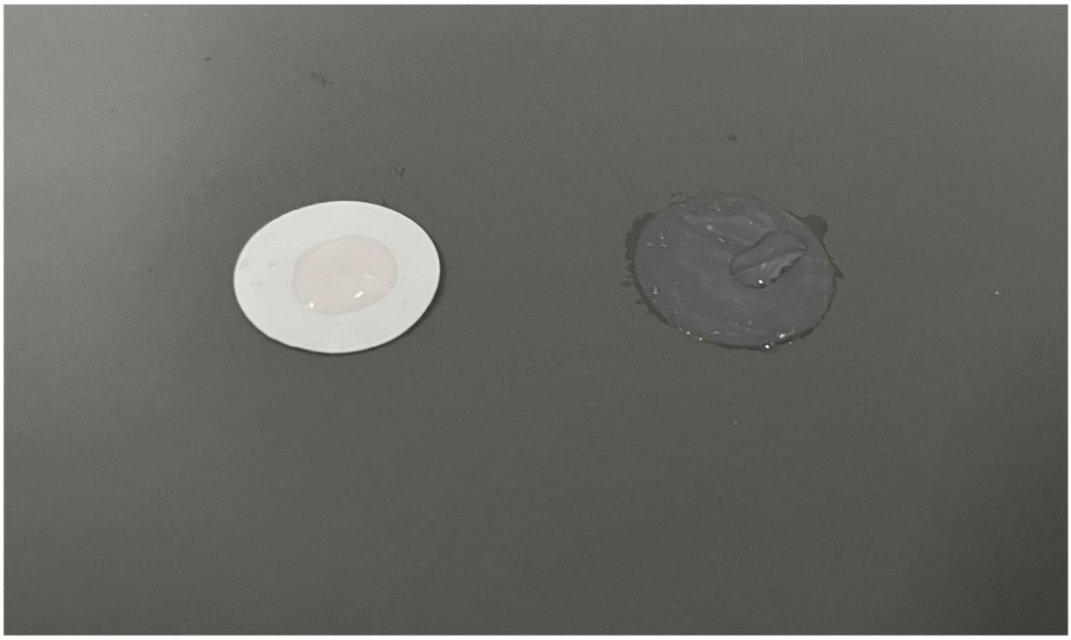

Figure S4. Wettability of LiDFOB-$LiBF_4$/SL (left) and LiDFOB-$LiBF_4$/SL-FB (right) toward polyethylene (PE) separator.

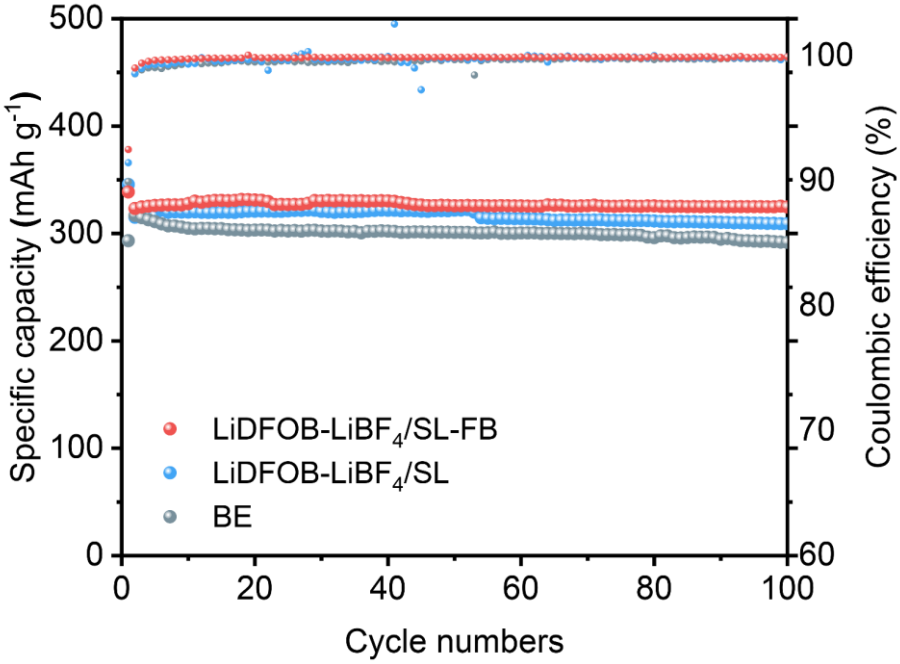

Figure S5. Cycling performance and Coulombic efficiency versus cycle number of Li||MCMB half-cells with various electrolytes at a constant rate (0.1C) between 0.005 V to 1.5 V.

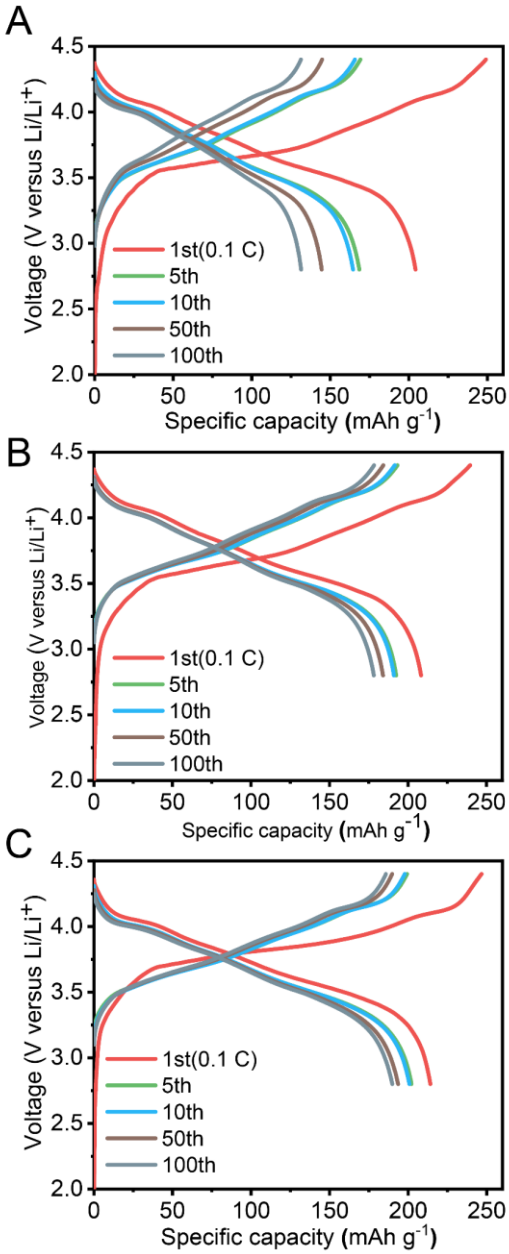

Figure S6. Voltage profiles of MCMB||NCM811 full-cells with BE (A), LiDFOB-$LiBF_4$/SL (B), and LiDFOB-$LiBF_4$/SL-FB (C) at a constant rate (0.5C) between 2.8 V to 4.4 V at 25 ℃.

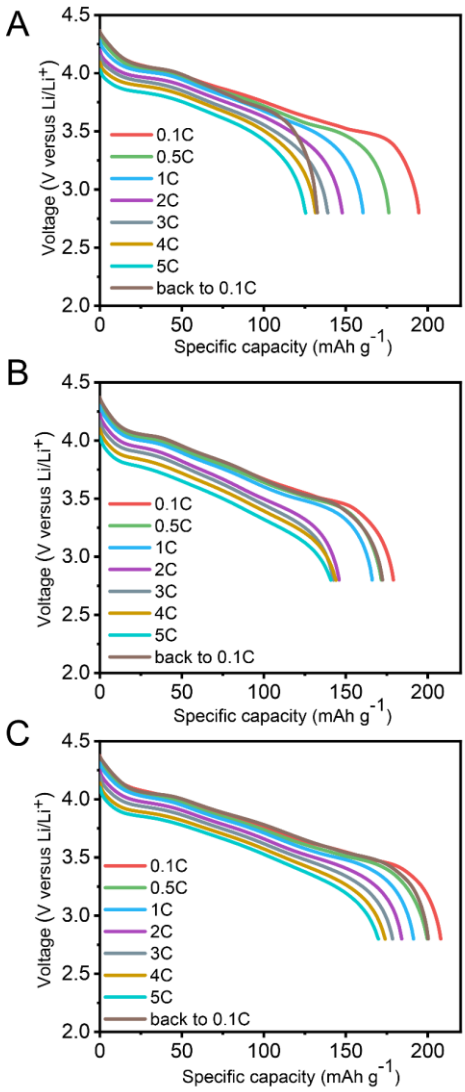

Figure S7. Discharge curves of MCMB||NMC811 full-cells using BE (A), LiDFOB-$LiBF_4$/SL (B), and LiDFOB-$LiBF_4$/SL-FB (C) under varying discharge rates (*x*C).

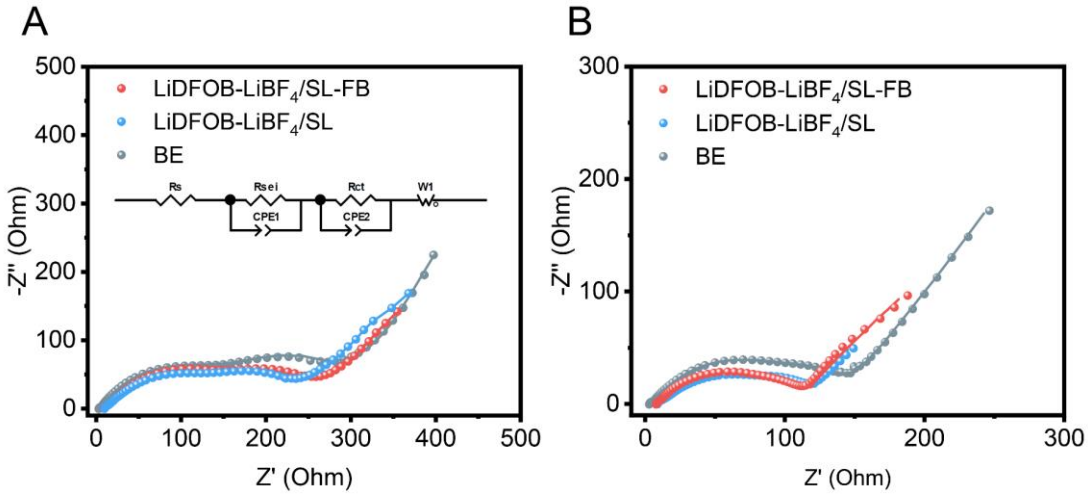

Figure S8. Electrochemical impedance spectra (EIS) measurements of MCMB||NCM811 full-cells after 10 cycles (A) and 50 cycles (B) with different electrolytes. The solid lines represent the fits results using an equivalent circuit shown in the Figure S8A.

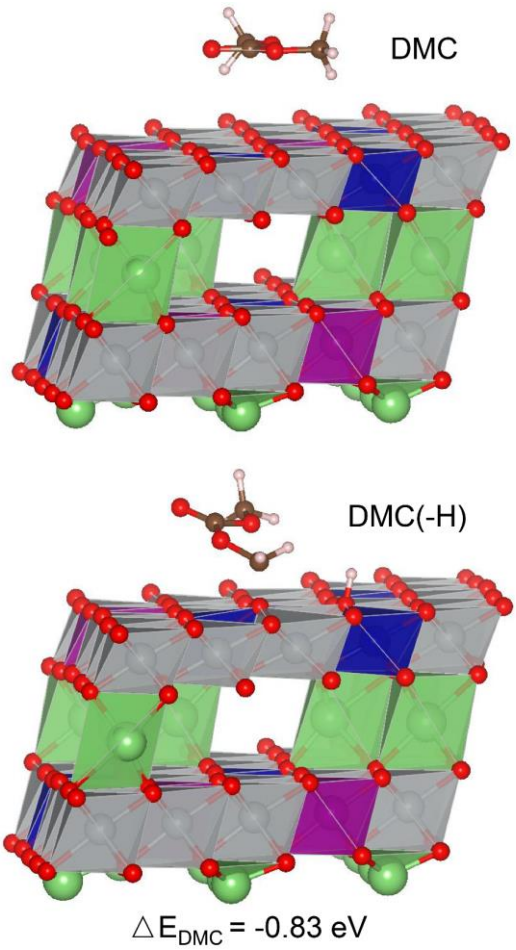

Figure S9. H-transfer reaction from DMC/DMC (-H) to the delithiated NCM811 (003) cathode surface from periodic DFT calculations.

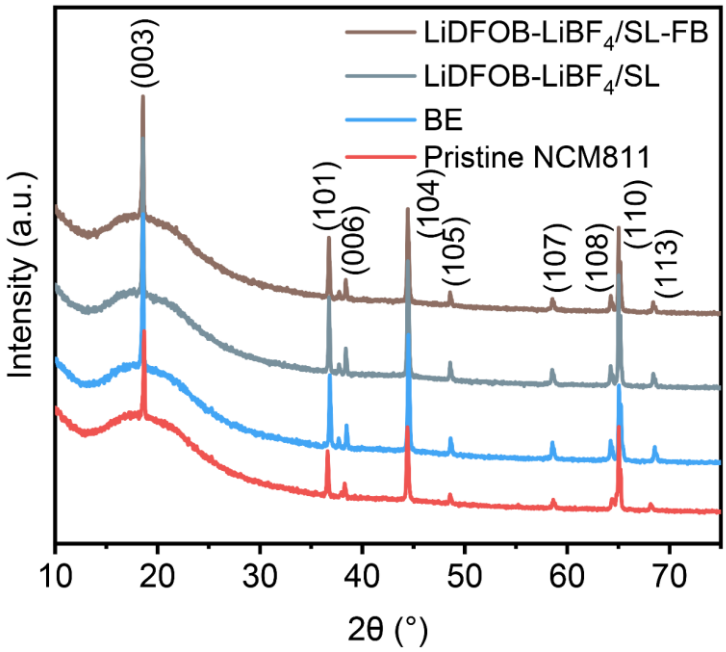

Figure S10. XRD patterns of uncycled pristine NCM811 cathode and cycled NCM811 cathodes recovered form MCMB||NCM811 full-cells after 50 cycles with different electrolytes.

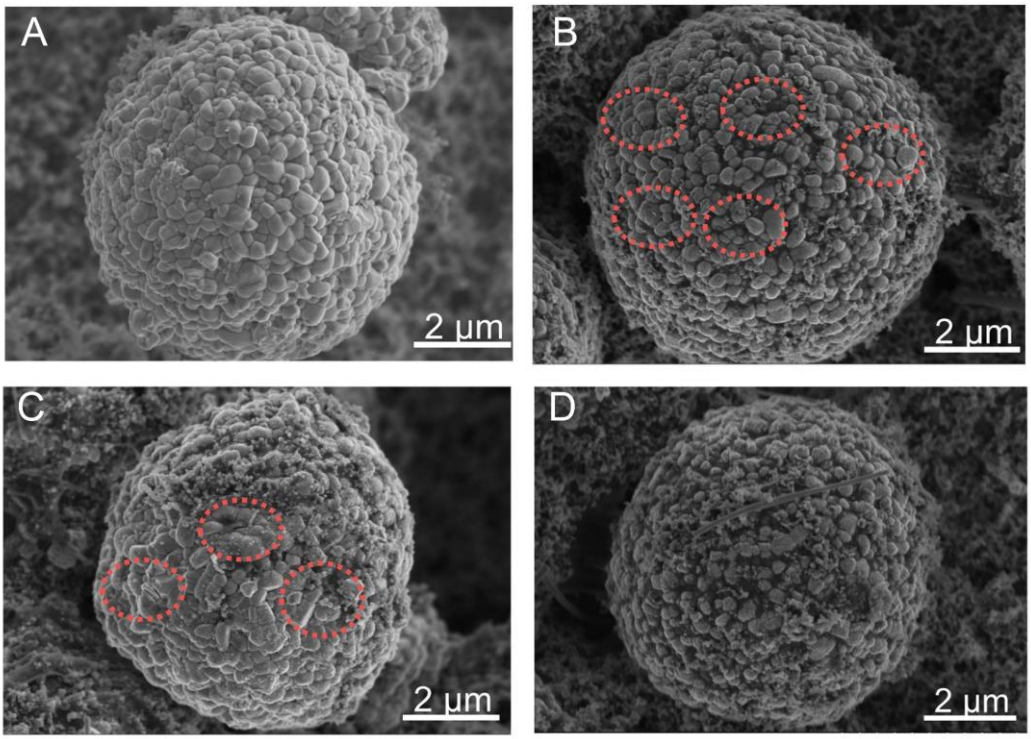

Figure S11. Typical SEM images of uncycled NCM811 electrode (A) and cycled NCM811 electrodes recovered from NCM811/MCMB full-cells after 50 cycles with BE (B), LiDFOB-$LiBF_4$/SL (C) and LiDFOB-$LiBF_4$/SL-FB (D), respectively.

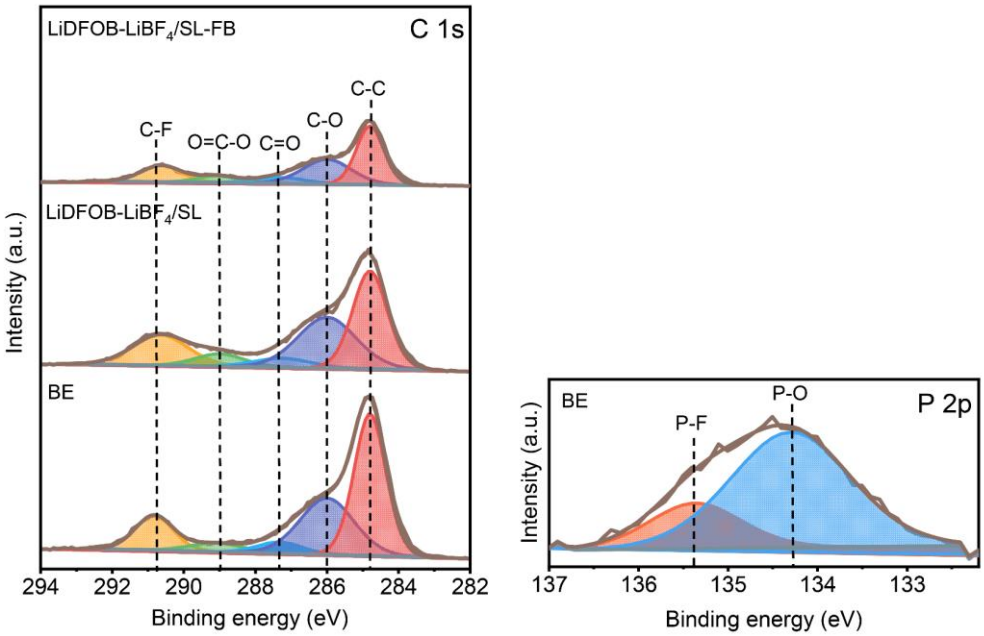

Figure S12. XPS C 1s, P 2p spectra for NCM811 cathodes recovered form MCMB||NCM811 full-cells after 50 cycles with various electrolytes.

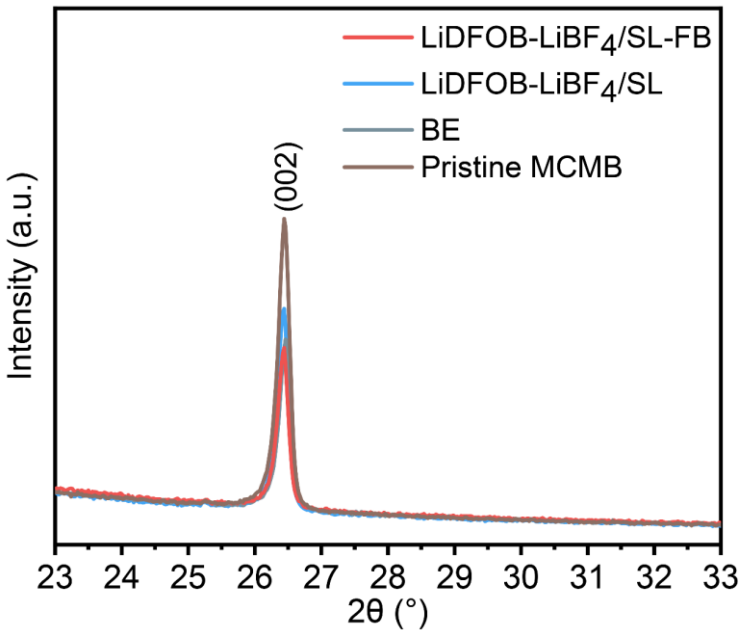

Figure S13. XRD patterns ((002) diffraction peak) of uncycled pristine MCMB anode and cycled MCMB anodes recovered form MCMB||NCM811 full-cells after 50 cycles with different electrolytes.

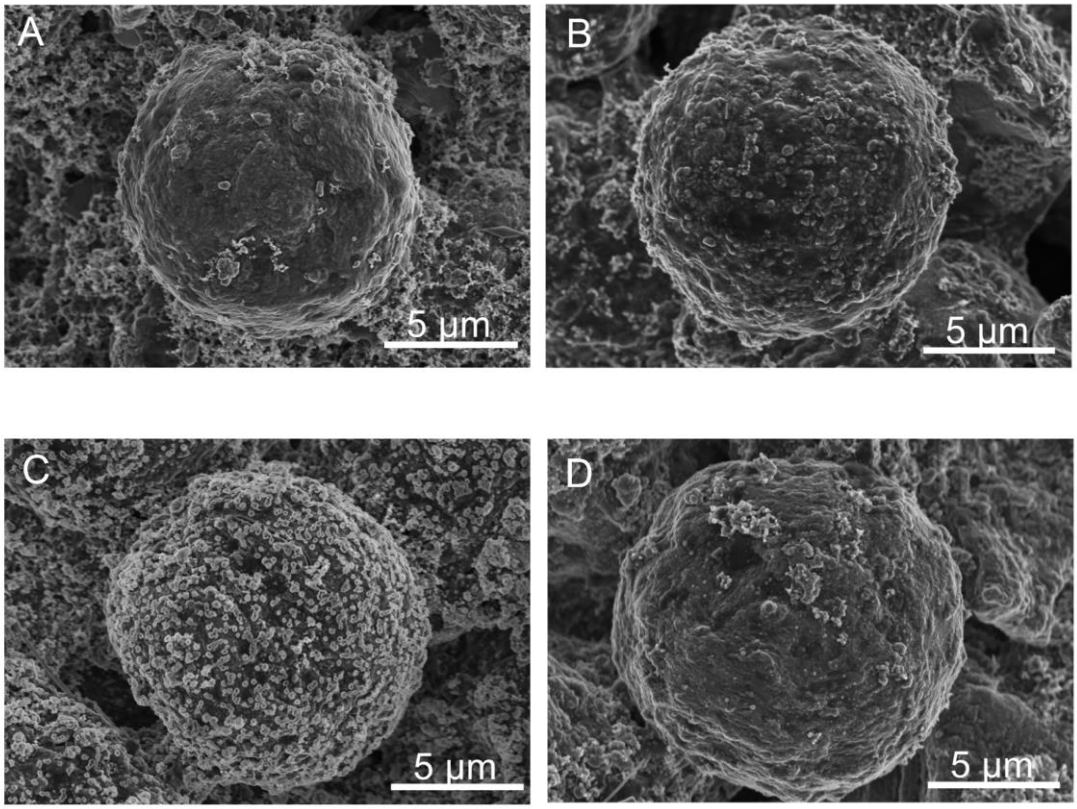

Figure S14. Typical SEM images of uncycled MCMB electrode (A) and cycled MCMB electrodes recovered from MCMB||NCM811 full-cells after 50 cycles with BE (B), LiDFOB-$LiBF_4$/SL (C) and LiDFOB-$LiBF_4$/SL-FB (D), respectively.

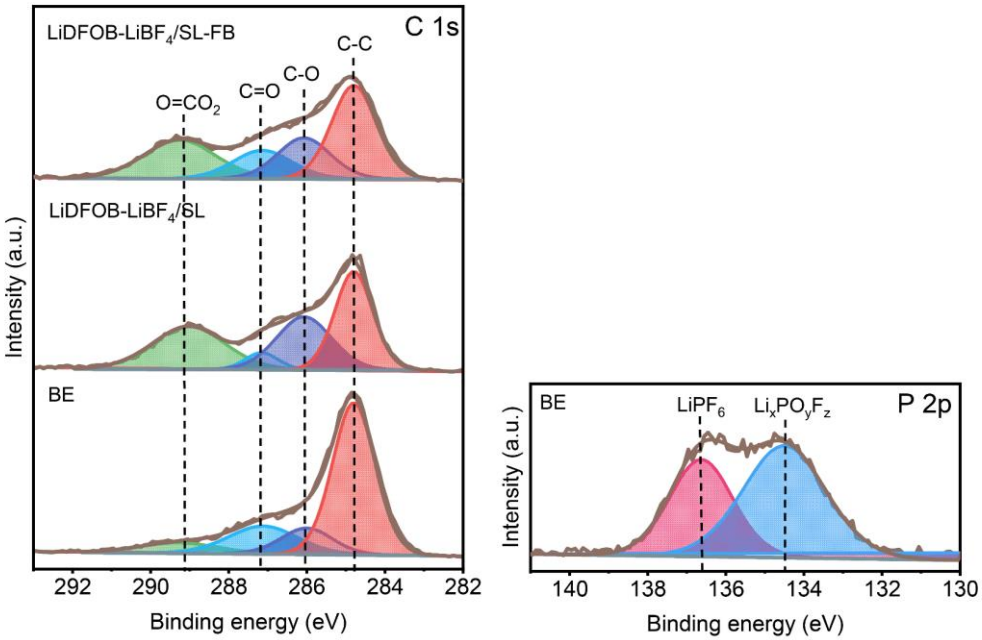

Figure S15. XPS C 1s, P 2p spectra for NCM811 cathodes recovered form MCMB||NCM811 full-cells after 50 cycles with various electrolytes.

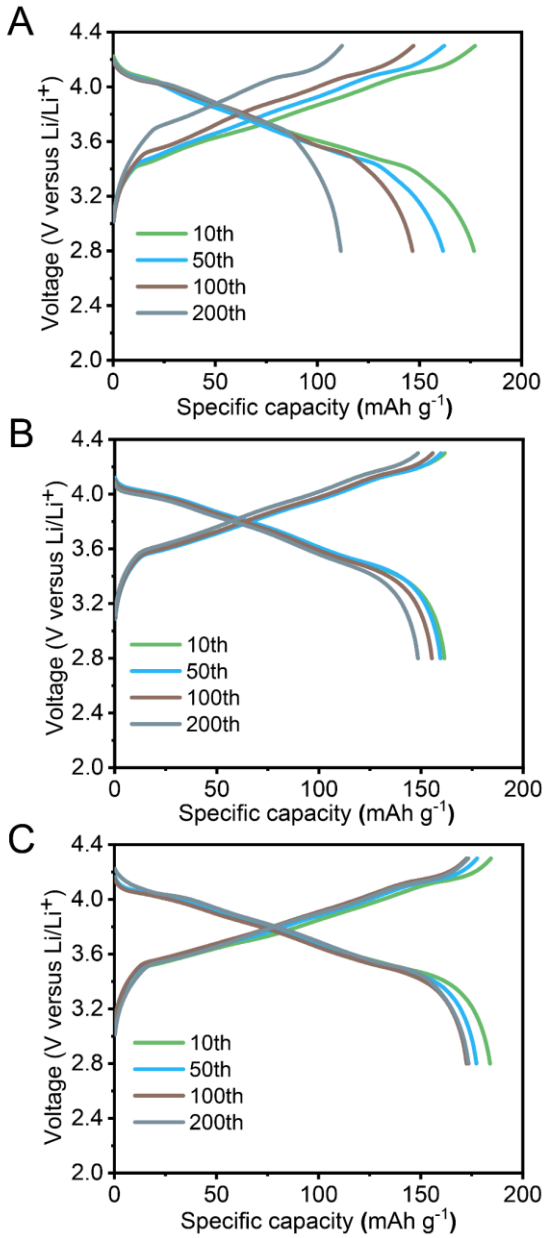

Figure S16. Voltage profiles of MCMB||NCM811 full-cells with BE (A), LiDFOB-$LiBF_4$/SL (B), and LiDFOB-$LiBF_4$/SL-FB (C) at a constant rate (0.5C) between 2.8 V to 4.3 V at 60 °C.